

# Maximum value of the pulse energy of a passively Q-switched laser as a function of the pump power

Jianlang Li, Ken-ichi Ueda, Jun Dong, Mitsuru Musha, and Akira Shirakawa

The finite recovery time  $T_s$  of the bleached absorber is presented as one of the possible mechanisms accounting for the increase–maximum–decrease in pulse energy  $E$  with the pumping rate  $W_p$  in cw-pumped passively Q-switched solid-state lasers, by analytically evaluating the sign of the derivative  $\partial E/\partial W_p$ . The results show that, in the low pump regime ( $T > T_s$ ,  $T$  is the interpulse period), the initial population density  $n_i$  remains constant, the final population density  $n_f$  decreases with  $W_p$ , and this results in a monotonic increase of  $E$  with  $W_p$ . In the high pump regime ( $T < T_s$ ),  $n_i$  decreases but  $n_f$  remains the same with  $W_p$ ; this results in a monotonic decrease of  $E$  with  $W_p$ . At the critical region ( $T \approx T_s$ ),  $E$  reaches its maximum value. A cw-pumped Yb:YAG laser passively Q switched by a Cr<sup>4+</sup>:YAG absorber is demonstrated to confirm this model. The theoretical model is also applied to the analysis of three previously reported passive Q switching solid-state [Nd:GdVO<sub>4</sub>, Nd<sup>+</sup>:LaSc<sub>3</sub>(BO<sub>3</sub>)<sub>4</sub> (Nd<sup>+</sup>:LSB), and Nd:YAG] lasers experiments. © 2006 Optical Society of America

OCIS codes: 140.3540, 140.3480, 140.3580.

## 1. Introduction

CW diode-pumped solid-state laser passively Q switched (PQS) by an intracavity saturable absorber (SA) is a common technique used to achieve short, high-peak-power laser pulses.<sup>1,2</sup> For several application, such as high-resolution imaging and ranging, high-energy pulses at high repetition rates are required. The knowledge of how the pump power affects the output pulse energy  $E$ , pulse width  $t_p$ , peak power  $P_{\text{peak}}$ , as well as the pulse repetition frequency (/rate) PRF, is essential.

The widely accepted conclusions<sup>3–6</sup> are based on Morris and Pollock's investigation<sup>2</sup> on the cw diode-pumped Nd:YAG laser passively Q switched by a LiF:F<sub>2</sub><sup>-</sup> color center. Their experiments show that, for a given value of the saturable loss, pulse energy and peak power, as well as pulse width, are kept essentially constants, while the pulse repetition frequency increases approximately linearly with pump power. Moreover, the authors suggest that  $E$  is primarily determined by the stored energy  $h\nu n_i$  in the gain medium ( $h\nu$  is the photon energy at laser wave-

length, while  $n_i$  is the initial inversion population density of gain medium), and the impact of pump power to  $n_i$  is negligible, so that the pulse energy remains constant as the pump power is varied.

However, it was recently observed, either in the cw-pumped Nd<sup>+</sup>:GdVO<sub>4</sub> laser PQS by Cr<sup>4+</sup>:YAG,<sup>7</sup> or in the cw-pumped Nd<sup>+</sup>:LaSc<sub>3</sub>(BO<sub>3</sub>)<sub>4</sub> (Nd<sup>+</sup>:LSB) microchip laser PQS by Cr<sup>4+</sup>:YAG,<sup>8</sup> that the pulse energy first increases with pump power, then reaches its maximum value before decreasing, while the PRF increases approximately linearly with pump power (see Fig. 8 in Ref. 7 and Fig. 2f in Ref. 8). The postulation was made in Ref. 7 that the increase of pulse energy with pump power results from the pump-induced indirect modification to initial inversion density,  $n_i$ , via thermal lensing and subsequent loss in the laser medium and absorber. Voitikov *et al.*<sup>8</sup> concluded that the reduction of the laser mode diameter results in the decrease of pulse energy with pump power. Another reported mechanism responsible for the decrease of pulse energy with pump power is the pump-induced bleaching of the saturable absorber in a PQS short-cavity microchip laser.<sup>9–11</sup> The increase of the effective unsaturated transmission of SA by the unabsorbed pump power results in higher pulse widths and lower pulse energies, especially when the pump light is nearly focused in the SA. Note that the above-mentioned mechanisms only account for monotonic variation (either only the increase or only the decrease) in pulse energy with pump power, and they

The authors are with the Institute for Laser Science, University of Electro-Communications, Tokyo 182-8585, Japan. J. Li's e-mail address is [j\\_li@ils.uec.ac.jp](mailto:j_li@ils.uec.ac.jp).

Received 23 January 2006; accepted 12 February 2006; posted 15 February 2006 (Doc. ID 67443).

0003-6935/06/215377-08\$15.00/0

© 2006 Optical Society of America

do not provide a comprehensive description of the observed increase–maximum–decrease in pulse energy with pump power. Moreover, the authors<sup>2,7,8</sup> do not address the effect of the pump power on the final inversion population  $n_f$ . Clearly, such effects should exist since the pulse energy  $E$  is proportional to the logarithm of  $n_i/n_f$ .<sup>4</sup>

Furthermore, the numerical results in Ref. 12 shows, that when the interpulse period  $T$  (inverse pulse repetition frequency, i.e.,  $T = 1/\text{PRF}$ ) is much smaller than the excited state lifetime  $\tau_s$  of the SA, i.e.,  $T \ll \tau_s$ ,  $E$  and  $P_{\text{peak}}$  decrease with pump power while both  $t_p$  and PRF increase with pump power. By using asymptotic methods and by numerically integrating the PQS laser rate equations, Peterson *et al.*<sup>13</sup> implicitly hinted the presence of respective extrema in the PQS pulse parameters with pump power. Namely, at low pump power above a lasing threshold,  $E$  and  $P_{\text{peak}}$  increase rapidly, whereas  $t_p$  decreases with pump power. When the pump power is increased further, these parameters reach some extrema, and then  $E$  and  $P_{\text{peak}}$  decrease rapidly whereas  $t_p$  increases. For any pump level, PRF always increases approximately linearly with pump power. The increase–maximum–decrease in  $E$  with pump power in Refs. 12 and 13 are obtained only under the numerical investigation of the simplified PQS laser rate equations, not related to the pump-dependent thermal lensing effect, pump-induced bleaching of SA, lasing manifolds, thermalization rate, and even the lower lasing level decay time.<sup>14</sup> This is quite different from the investigations in Refs. 2, 7, and 8.

In this paper, based on the acknowledged conclusion that inverse  $T$  nearly linearly increases with the pump rate (i.e.,  $1/T \propto W_p$ ), we consider the finite recovery time of the bleached saturable absorber as another possible mechanism explaining the existence of maximum pulse energy as the pump power is varied. The main objective of this paper is whether the competition between interpulse period  $T$  and finite recovery time of the saturable absorber plays the dominant role for the extrema phenomena in the pulse parameters (pulse energy  $E$ , peak power  $P_{\text{peak}}$ , and pulse width  $t_p$ ).

In Section 2, we summarize the solutions to the PQS laser rate equations. In Section 3, by defining a time scale—“the finite recovery time”  $T_s$  of SA—and comparing it with  $T$  ( $T > T_s$ ,  $T < T_s$ , and  $T \approx T_s$ ), we evaluate analytically the sign of the derivative  $\partial E/\partial W_p$  (positive, zero, or negative) and then determine the conditions in which the pulse energy  $E$  either increases, reaches its maximum or decreases with pumping rate  $W_p$ . In Section 4, we compare the conclusions with our experimental results and those reported in the literature, and revisit Morris and Pollock’s conclusion in the light of our model.

## 2. Laser Rate Equations (Theoretical Background)

We treat the gain medium and the saturable absorber as ideal four-level and two-level systems, respectively, and concentrate on the main physical mechanism presented in the well-established model,<sup>3–6,12,13</sup>

without including the effect of lasing manifolds, thermalization among the energy levels of the gain medium,<sup>14</sup> and the excited state absorption<sup>5</sup> of the absorber. The coupled rate equations for a cw-pumped passively  $Q$ -switched laser are written in the following form<sup>3–6,12,15,16</sup>:

$$d\phi/dt = \phi[2\sigma nl - 2\sigma_s n_s l_s - \ln(1/R) - L]/t_r, \quad (1a)$$

$$dn/dt = -\gamma\sigma n c\phi - n/\tau_{21} + W_p(N_t - n), \quad (1b)$$

$$dn_s/dt = -\gamma_s\sigma_s c n_s \phi + (n_{s0} - n_s)/\tau_s. \quad (1c)$$

Here,  $N_t$  is the doping concentration of the gain medium,  $n$  is the inversion population density,  $\sigma$  is the stimulated emission cross section,  $l$  is gain length,  $\tau_{21}$  is the decay time of upper energy level, and  $\gamma = 1$  is inversion reduction factor.  $n_{s0}$  is the total doping concentration of SA,  $n_s$  is the population density on its ground state,  $\tau_s$  is the decay time,  $\sigma_s$  is absorption cross section at lasing wavelength,  $l_s$  is its length,  $\gamma_s = 2$  is absorption reduction factor.  $\phi$  is the photon density in the cavity,  $W_p$  is the pumping rate,  $t_r$  is the round-trip time of laser cavity,  $L$  is the nonuseful dissipative loss per round,  $R$  is the reflectivity of the out coupler, and  $c$  is the speed of light.

For the convenience of the further discussion, the solutions<sup>4–6</sup> of Eqs. (1a)–(1c) are directly cited and summarized herein by considering the PQS operation as consisting of the following two stages.<sup>17</sup>

### A. Pumping Cycle

In this stage, there are no lasing photons inside the resonator,  $\phi = 0$ . The population density on the ground state of the absorber and the accumulations of the inversion population density of gain medium between the two successive pulses are given by<sup>4,6</sup>

$$n_{si} = n_{s0} - (n_{s0} - n_{sf})e^{-T/\tau_s}, \quad (2a)$$

$$n_i = \frac{W_p\tau_{21}N_t}{1 + W_p\tau_{21}} - \left( \frac{W_p\tau_{21}N_t}{1 + W_p\tau_{21}} - n_f \right) e^{-(1+W_p\tau_{21})T/\tau_{21}}. \quad (2b)$$

Here,  $n_f$  is the final inversion population density of active medium left over by previous pulse at the start of current pump cycle for repetitive  $Q$  switching, and  $n_i$  is the initial inversion population density at the start of  $Q$  switching.  $n_{sf}$  is the final population density of the absorber’s ground state left over by previous pulse, at the start of the current pump cycle,  $n_{si}$  is the initial population density of the absorber’s ground state at the start of  $Q$  switching.  $T$ , the interpulse period, is the time duration for the pumping cycle between the end point of previous pulse and the start point of the next pulse,  $T = 1/\text{PRF}$ .

By applying the bleached approximation condition<sup>13</sup>  $n_{sf} \ll n_{s0}$  to Eq. (2a), solving  $T$  in Eq. (2a), and substituting it into Eq. (2b), Eqs. (2a) and 2(b) take the following forms:

$$n_{si} \approx n_{s0}[1 - \exp(-T/\tau_s)], \quad (3a)$$

$$\begin{aligned} n_f &= \frac{W_P \tau_{21} N_t}{1 + W_P \tau_{21}} - \left( \frac{W_P \tau_{21} N_t}{1 + W_P \tau_{21}} - n_i \right) \\ &\quad \times \left( \frac{n_{s0} - n_{si}}{n_{s0} - n_{sf}} \right)^{-(\tau_s/\tau_{21})(1+W_P \tau_{21})}, \\ &\approx \frac{W_P \tau_{21} N_t}{1 + W_P \tau_{21}} - \left( \frac{W_P \tau_{21} N_t}{1 + W_P \tau_{21}} - n_i \right) \\ &\quad \times \left( 1 - \frac{n_{si}}{n_{s0}} \right)^{-(\tau_s/\tau_{21})(1+W_P \tau_{21})}. \end{aligned} \quad (3b)$$

Here, Eq. (3b) reflects the relation constraining the gain medium parameter ( $n_i$ ,  $n_f$ ,  $\tau_{21}$ ) and absorber parameter ( $n_{si}$ ,  $\tau_s$ ) through pumping rate  $W_P$  during the pumping cycle.

### B. Pulsing Stage ( $\phi = 0$ )

In this stage, the terms of pump and spontaneous decay in Eqs. (1b) and (1c) are neglected because of the fast and intense pulse. The solutions to the modified coupled equations satisfy<sup>4</sup>

$$2\sigma n_f l - 2\sigma_s n_{si} l_s - \ln(1/R) - L = 0, \quad (4a)$$

$$\ln \frac{n_i}{n_f} = \frac{2\sigma l}{\ln\left(\frac{1}{R}\right) + L} \left\{ n_i - n_f - \frac{l_s}{l} \frac{\gamma}{\gamma_s} n_{si} \left[ 1 - \left( \frac{n_f}{n_i} \right)^\alpha \right] \right\}, \quad (4b)$$

where the constant parameter  $\alpha = \gamma_s \sigma_s / \sigma \gamma^4$ . Equation (4a) states that the round-trip gain is exactly equal to the round-trip loss before pulsing occurs. The transcendental equation Eq. (4b) shows the relation constraining the active medium parameters ( $n_i$ ,  $n_f$ ,  $\gamma$ , and  $\sigma$ ) and the absorber parameter ( $n_{si}$ ,  $\gamma_s$ , and  $\sigma_s$ ) through  $\alpha$  during the pulsing stage.

The expression of total output pulse energy  $E$  of the Q-switched pulse is given by<sup>3,4</sup>

$$E = h\nu A / (2\sigma\gamma) \ln(1/R) \ln(n_i/n_f), \quad (5)$$

which shows that the pulse energy not only is primarily determined by the initial inversion population density  $n_i$  (the stored energy on the gain medium is  $h\nu n_i$ ) before each pulse, but also by the final inversion population density  $n_f$  left over at the start of next pumping cycle for repetitive Q switching.

In Section 3, Eq. (5), with the combination of Eqs. (3a) and (3b), and (4a) and (4b), would be applied to analyze the sign of  $\partial E / \partial W_P$ .

### 3. Pump-Dependent Pulse Energy

The criterion for clarifying the monotony of the function relation  $E \sim W_P$  is whether  $\partial E / \partial W_P$  is positive, zero, or negative with  $W_P$ . Taking the first derivative

of Eq. (5) with respect to the pumping rate  $W_P$ , we obtain

$$\frac{\partial E}{\partial W_P} = \frac{h\nu A}{2\sigma\gamma} \ln\left(\frac{1}{R}\right) \frac{1}{n_f} \left( \frac{n_f}{n_i} \frac{\partial n_i}{\partial W_P} - \frac{\partial n_f}{\partial W_P} \right). \quad (6)$$

Taking the first derivative of Eqs. (4a) and (4b) with respect to the pumping rate  $W_P$ , we obtain

$$\partial n_{si} / \partial W_P = \sigma l / (\sigma_s l_s) \partial n_i / \partial W_P, \quad (7a)$$

$$\begin{aligned} \frac{1}{n_f} \left( \frac{n_f}{n_i} \frac{\partial n_i}{\partial W_P} - \frac{\partial n_f}{\partial W_P} \right) &= \frac{2\sigma l}{\ln(1/R) + L} \left\{ \frac{\partial n_i}{\partial W_P} - \frac{\partial n_f}{\partial W_P} \right. \\ &\quad - \frac{l_s}{l} \frac{\gamma}{\gamma_s} \left[ 1 - \left( \frac{n_f}{n_i} \right)^\alpha \right] \frac{\partial n_{si}}{\partial W_P} \\ &\quad - \frac{l_s}{l} \frac{\gamma}{\gamma_s} n_{si} \alpha \left( \frac{n_f}{n_i} \right)^\alpha \\ &\quad \left. \times \frac{1}{n_f} \left( \frac{n_f}{n_i} \frac{\partial n_i}{\partial W_P} - \frac{\partial n_f}{\partial W_P} \right) \right\}. \end{aligned} \quad (7b)$$

The underlined terms in Eqs. (6) and (7b) are the same; hence, with the combination of Eqs. (6) and (7a), Eq. (7b) can be expressed in the form of the derivative  $\partial E / \partial W_P$  by

$$\frac{\partial E}{\partial W_P} = \frac{h\nu A}{2\sigma\gamma} \ln\left(\frac{1}{R}\right) \frac{\left[ 1 - \frac{1}{\alpha} + \frac{1}{\alpha} \left( \frac{n_f}{n_i} \right)^\alpha \right] \frac{\partial n_i}{\partial W_P} - \frac{\partial n_f}{\partial W_P}}{\frac{2\sigma l}{\ln(1/R) + L} + \frac{l_s \gamma}{l \gamma_s} n_{si} \alpha \left( \frac{n_f}{n_i} \right)^\alpha}. \quad (8)$$

Both Eqs. (6) and (8) represent the derivative of  $E$  with respect to  $W_P$ , and would be treated equally in evaluating the sign of  $\partial E / \partial W_P$ .

During the pumping cycle, the recovery of bleached absorber and the accumulation of the inversion population density in gain medium are independent of each other before satisfying the threshold condition Eq. (4a). The interpulse period  $T$  is associated with the pump power by the relation that inverse  $T$  nearly linearly increases with pump power, i.e.,  $1/T \propto W_P$ . Here we define the full recovery time of the saturable absorber as  $T_s$ , which is the duration that takes the absorber decay from the bleached state to its equilibrium and varies within a wide region (the further description of  $T_s$  is given in Subsection 3.D). By comparing constant  $T_s$  with  $T$ , we can divide PQS behavior into two regimes: the low pump regime ( $T > T_s$ ; the large  $T$  corresponds to low pumping rate) and high pump regime ( $T < T_s$ ; the pumping rate is high), separated by the critical region ( $T \approx T_s$ ).

### A. Low Pump Regime

In this regime,  $T > T_s$ , the low pumping rate results in that the buildup of the inversion density is slower than the full recovery of bleached SA. Hence  $n_{si}$  in Eq. (3a) is the constant very close to  $n_{s0}$ , i.e.,  $n_{si} \approx n_{s0}$ . After substituting  $n_{si} \approx n_{s0}$  into Eq. (4a),  $n_i$  is determined by

$$n_i \approx [2\sigma_g n_{s0} l_s + \ln(1/R) + L] / (2\sigma l). \quad (9)$$

The constant  $n_{si}$  and  $n_i$  result in

$$\partial n_{si} / \partial W_P \approx 0, \quad (10a)$$

$$\partial n_i / \partial W_P \approx 0. \quad (10b)$$

By taking the first derivative of Eq. (3b) with respect to  $W_P$ , and thereafter substituting Eqs. (10a) and (10b) into it, we obtain

$$\begin{aligned} \frac{\partial n_f}{\partial W_P} = & \frac{N_t \tau_{21}}{(1 + W_P \tau_{21})^2} \left[ 1 - \left( 1 - \frac{n_{si}}{n_{s0}} \right)^{-(\tau_s/\tau_{21})(1 + W_P \tau_{21})} \right] \\ & + \tau_s \left( \frac{W_P N_t \tau_{21}}{1 + W_P \tau_{21}} - n_i \right) \\ & \times \left( 1 - \frac{n_{si}}{n_{s0}} \right)^{-(\tau_s/\tau_{21})(1 + W_P \tau_{21})} \ln \left( 1 - \frac{n_{si}}{n_{s0}} \right). \quad (11) \end{aligned}$$

Note that  $n_{si}$  is the constant very close to, but nevertheless still less than  $n_{s0}$ ; this results in the terms in Eq. (11) satisfying the relations as follows:

$$\left( 1 - \frac{n_{si}}{n_{s0}} \right)^{-(\tau_s/\tau_{21})(1 + W_P \tau_{21})} > 1, \quad (12a)$$

$$\ln \left( 1 - \frac{n_{si}}{n_{s0}} \right) < 0. \quad (12b)$$

According to Eqs. (34) and (38) in Ref. 4, we also have

$$W_P N_t \tau_{21} / (1 + W_P \tau_{21}) \geq n_i. \quad (13)$$

The left term of Eq. (13) represents the small-signal inversion population at steady state under the pumping rate  $W_P$ . Therefore both the first and second terms of the right-hand side in Eq. (11) are also negative. Therefore we obtain

$$\partial n_f / \partial W_P < 0. \quad (14)$$

With the results from Eqs. (10b) and (14), the derivative expression in Eq. (6) is given by

$$\frac{\partial E}{\partial W_P} = - \frac{h\nu A}{2\sigma\gamma} \ln \left( \frac{1}{R} \right) \frac{1}{n_f} \frac{\partial n_f}{\partial W_P} > 0. \quad (15)$$

Therefore as seen from Eqs. (14) and (15), in the low pump regime, even though  $n_i$  remains constant,  $n_f$  decreases with  $W_P$ , the energy utilization factor<sup>15,16</sup>

$n_i/n_f$ , and also the coupled pulse energy increases with the pumping rate. Nevertheless in previous treatments,<sup>2,7,8</sup> the effect of pumping rate on  $n_f$  is neglected.

Equation (15) shows the generalized variation of the pulse energy with a pumping rate in the low pumping rate. In one special case of Eq. (15),  $W_P \tau_{21} \ll 1$ , which is usually valid for most four-level laser systems, Eq. (3b) can be approximated as

$$n_f \approx W_P \tau_{21} N_t - (W_P \tau_{21} N_t - n_i) (1 - n_{si}/n_{s0})^{-\tau_s/\tau_{21}}. \quad (16)$$

Further, the derivative of  $n_f$  with respect to  $W_P$  is given by

$$\frac{\partial n_f}{\partial W_P} \approx N_t \tau_{21} [1 - (1 - n_{si}/n_{s0})^{-\tau_s/\tau_{21}}], \quad (17)$$

and correspondingly,

$$\begin{aligned} \frac{\partial E}{\partial W_P} = & - \frac{h\nu A}{2\sigma\gamma} \ln \left( \frac{1}{R} \right) \frac{1}{n_f} \frac{\partial n_f}{\partial W_P} \\ \approx & - \frac{h\nu A}{2\sigma\gamma} \ln \left( \frac{1}{R} \right) \frac{1}{n_f} N_t \tau_{21} \left[ 1 - \left( 1 - \frac{n_{si}}{n_{s0}} \right)^{-\tau_s/\tau_{21}} \right], \quad (18) \end{aligned}$$

which is an approximation expression of  $\partial E / \partial W_P$  in the case of  $W_P \tau_{21} \ll 1$ . It is seen, when  $W_P \tau_{21} \ll 1$ , the positive value of  $\partial E / \partial W_P$ , depends not only the total dopant concentration  $N_t$ , the final population density  $n_f$  of active medium, the output coupler's reflectivity  $R$ , but also the ratio  $\tau_s/\tau_{21}$ . The effect of this ratio on the positive  $\partial E / \partial W_P$  for different absorbers when  $W_P \tau_{21} \ll 1$  will be discussed in Section 5.

### B. Critical Region

At this region, the corresponding pumping rate is represented in the temporal domain by  $T \approx T_s$ , where the buildup time of  $n_i$  rightly approaches the absorber's full recovery time  $T_s$ . The value of  $\partial E / \partial W_P$  at the critical region will be given in Subsection 3.D.

### C. High Pump Regime

In this regime  $T < T_s$ , the high pumping rate results in the fast energy storage in the gain medium, and the bleached SA does not recover to its equilibrium state before  $Q$  switching, i.e.,  $n_{si} < n_{s0}$ . Because  $1/T$  is proportional to  $W_P$ , and  $n_{si}$  in Eq. (3a) is proportional to  $T$ , we have  $n_{si} \propto 1/W_P$ ,  $n_{si}$  decreases with pumping rate  $W_P$ , so that

$$\partial n_{si} / \partial W_P < 0. \quad (19)$$

According to Eqs. (7a) and (19), we easily get

$$\partial n_i / \partial W_P < 0. \quad (20)$$

As seen in Eq. (6), the sign of  $\partial E / \partial W_P$  depends on both  $\partial n_i / \partial W_P$  and  $\partial n_f / \partial W_P$ . Due to  $\partial n_i / \partial W_P \neq 0$ , there-

fore after comparing the coefficients of the term  $\partial n_i / \partial W_p$  in the numerator and denominator of Eqs. (6) and (8), we could have

$$\frac{1 - \frac{1}{\alpha} + \frac{1}{\alpha} \left(\frac{n_f}{n_i}\right)^\alpha}{\frac{\ln(1/R) + L}{2\sigma l} + \frac{l_s \gamma}{l \gamma_s} n_{si} \alpha \left(\frac{n_f}{n_i}\right)^\alpha} = \frac{n_f}{n_i} \frac{1}{n_f}. \quad (21)$$

Similarly, comparing the term of  $\partial n_f / \partial W_p$  in Eqs. (6) and (8), we obtain

$$\frac{1}{\frac{\ln(1/R) + L}{2\sigma l} + \frac{l_s \gamma}{l \gamma_s} n_{si} \alpha \left(\frac{n_f}{n_i}\right)^\alpha} \frac{\partial n_f}{\partial W_p} = \frac{1}{n_f} \frac{\partial n_f}{\partial W_p}. \quad (22)$$

During the PQS operation,  $0 < n_f/n_i < 1$  and  $\alpha = \gamma_s \sigma_s / \sigma \gamma > 1$ , so that there always exists the following absolute inequality relation between the two related terms at the left side and right side of Eq. (21); that is,

$$\left(1 - \frac{1}{\alpha}\right) + \frac{1}{\alpha} \left(\frac{n_f}{n_i}\right)^\alpha > \frac{n_f}{n_i}. \quad (23)$$

From this absolute inequality of Eqs. (23) and (21), it is derived that

$$\frac{1}{\frac{\ln(1/R) + L}{2\sigma l} + \frac{l_s \gamma}{l \gamma_s} n_{si} \alpha \left(\frac{n_f}{n_i}\right)^\alpha} < \frac{1}{n_f}. \quad (24)$$

Comparing the coefficients of the term  $\partial n_f / \partial W_p$  on both sides of Eqs. (22) with the terms in both sides of inequality Eq. (24), we get the following result:

$$\partial n_f / \partial W_p = 0. \quad (25)$$

After substituting Eqs. (20) and (25) into Eq. (7), the sign of  $\partial E / \partial W_p$  is given by

$$\frac{\partial E}{\partial W_p} = \frac{h\nu A}{2\sigma\gamma} \ln\left(\frac{1}{R}\right) \frac{1}{n_i} \frac{\partial n_i}{\partial W_p} < 0. \quad (26)$$

Here the negative  $\partial E / \partial W_p$  shows that, in the high pump regime,  $n_i$  decreases, whereas  $n_f$  remains constant with the pumping rate, and pulse energy  $E$  decreases monotonously with  $W_p$ .

#### D. Determination of the Full Recovery Time $T_s$ of the Bleached Absorber

First we summarized the analytical results in Subsections 3.A and 3.C. In the low pump regime where the interpulse period  $T$  is larger than  $T_s$ ,  $n_i$  remains constant while  $n_f$  decreases with  $W_p$ . This results in a monotonic increase of  $E$  with  $W_p$ . Inversely, in the high pump regime where  $T$  is smaller than  $T_s$ ,  $n_i$

decreases while  $n_f$  remains constant with  $W_p$ ; this results into a monotonic decrease of  $E$  with  $W_p$ .

Considering the continuity of  $E$  as the function of  $W_p$ , at critical region, or the transitional region between the low pump and high pump regimes where the interpulse period  $T$  is around  $T_s$ , one should have

$$\partial E / \partial W_p = 0. \quad (27)$$

This means the maximum value of pulse energy  $E$  could be represented by the repetition rate at  $f_s \approx 1/T_s$ . It is the area where designers should aim at for the applications when the high pulse energy is important.

Further, the physical meaning of  $T_s$  needs to be clarified. Let  $n_s$  be the population density on the absorber's ground state due to the exponential decay of the bleached absorber, and it is determined by

$$n_s = n_{s0}(1 - e^{-t/\tau_s}), \quad (28)$$

where  $t$  is the time. For the ideal case of the two-level absorber, the full recovery of the bleached absorber requires  $n_s = n_{s0}$  when  $t = T_s$  in Eq. (28), which means the full recovery time  $T_s \rightarrow \infty$  mathematically.

Therefore to discriminate the  $T_s$  applied in our paper from the infinity, it is necessary to point out the following two aspects. First, here  $T_s$  is some finite value (or range) larger than  $\tau_s$ , which keeps Eqs. (10a) and (10b) valid for low pump regime ( $T > T_s$ ), and then Eqs. (19) and (20) valid for high pump regime ( $T < T_s$ ). Second, in the pulsing stage and the pumping cycle, the absorber undergoes the sustaining illumination of the amplified spontaneous emission<sup>18,19</sup> (ASE) and/or the unabsorbed pump power.<sup>9–11</sup> Such illuminations are actually time dependent<sup>19</sup> because of the time-dependent population inversion in gain medium. They not only impel the bleaching of the absorber during the pulsing stage,<sup>10,11</sup> but also always induce the nonzero equilibrium population on the excited state of the absorber during the recovery of the bleached absorber, and thus dwarf the recovery time and results in a finite recovery time  $T_s$ .

#### 4. Experiments and Related Comparisons

The experimental setup is shown in Fig. 1. The beam of a fiber-coupled 940 nm diode laser is collimated and tightly focused (10 at. % Yb-doped YAG ceramics). The Yb:YAG has the size  $10 \times 10 \times 1$  mm (thickness), is coated for antireflection at 940 nm and high reflection at 1030 nm on its front surface, and coated for antireflection at both 940 and 1030 nm on the rear surface. The absorption coefficient at the pump wavelength for our Yb:YAG ceramics is  $\sim 10 \text{ cm}^{-1}$ . The comparison of ceramic lasers with single crystal materials is given in Ref. 20. The Yb:YAG ceramics sample is held between two copper plates for conductive cooling. The central parts of two copper plates are perforated with 2 mm diameter apertures for beam transmission. The uncoated  $\text{Cr}^{4+}$ :YAG ceramic is 0.3 nm thick, with initial transmission  $T_0 = 94\%$ ,

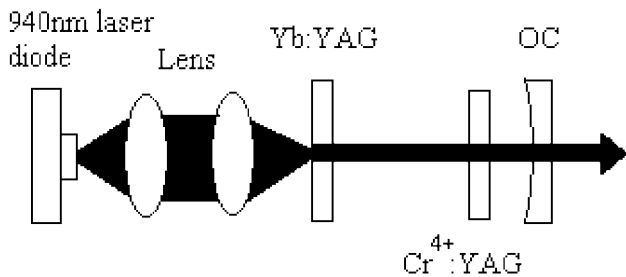


Fig. 1. The experimental setup of passive Q-switched Yb:YAG/Cr<sup>4+</sup>:YAG ceramics laser. OC, output coupler.

placed parallel to the Yb:YAG and close to the output coupler without any cooling. The radius of curvature of output concave mirror is 70 mm with 95% reflectivity at 1030 nm. The stable TEM<sub>00</sub> mode output is obtained when the laser cavity length is approximately 60 mm. The output power and the pulse form are monitored by a powermeter, a high-speed InGaAs photodetector and Tektronix 500 MHz digital oscilloscope, respectively.

The measured pulse parameters (average power  $P_{ave}$ , pulse width  $t_p$ , pulse repetition frequency PRF, pulse energy  $E$ , and peak power  $P_{peak}$ ) are plotted as functions of the absorbed pump power  $P_{abs}$  in Fig. 2.

As seen from Fig. 2(a), the lasing threshold is about 270 mW, and average power  $P_{ave}$  is linearly proportional to the absorbed pump power  $P_{abs}$ , with 21% slope efficiency. Pulse repetition frequency increases with the absorbed pump power. When the absorbed pump power reaches the maximum value  $P_{abs} = 1047$  mW, PRF is 47 KHz, the corresponding  $P_{ave}$  is 177 mW. Figure 2(b) shows the relation of pulse duration and peak power with the absorbed pump power. As pump increases, the pulse width shows a minimum value  $t_p = 15.6$  ns, whereas the peak power shows a maximum value  $P_{peak} = 540$  W approximately at  $P_{abs} = 585$  mW; Fig. 2(c) shows the function relation of pulse energy with the absorbed pump power. When the absorbed pump power  $P_{abs} < 585$  mW,  $E$  increases to 8.55  $\mu$ J with  $P_{abs}$ . When  $P_{abs} > 585$  mW,  $E$  decreases to 3.76  $\mu$ J with  $P_{abs}$ .

From the results above, the increase–maximum–decrease in pulse energy with pump power is already observed. The maximum value of pulse energy, 8.55  $\mu$ J when absorbed pump power  $P_{abs} = 585$  mW, corresponds to 8 kHz pulse repetition frequency.

## 5. Discussions

### A. Analyses to the Related Investigations

Here we recall the observed increase–maximum–decrease of the pulse energy with pump power reported in Refs. 7 and 8. Figures 5 and 8 in Ref. 7 represent the function relations of the measured PRF and  $E$  with pump power, respectively, in a cw-pumped Nd<sup>+</sup>:GdVO<sub>4</sub> laser passively Q switched by Cr<sup>4+</sup>:YAG crystal. Seen from these two figures, the maximum value of pulse energy 90  $\mu$ J corresponds to

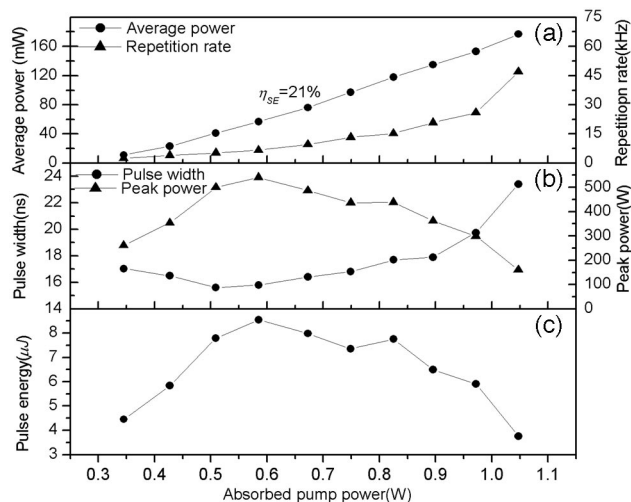


Fig. 2. The measured pulse parameters of PQS Cr:YAG/Yb:YAG ceramics laser as a function of absorbed pump power: (a) Average power and repetition rate, (b) pulse duration and peak power, and (c) pulse energy, when the output coupling  $R = 95\%$ .

9.3 W absorbed pump power and 33 kHz pulse repetition frequency. When the absorbed pump power is smaller than 9.3 W or PRF < 33 kHz,  $E$  increases with pump power. When absorbed pump power is larger than 9.3 W or PRF > 33 kHz,  $E$  starts to decrease with pump power. The pulse repetition frequency corresponding to the maximum value of pulse energy is 33 kHz. It is concluded that the reduction of the laser mode diameter with the pump power accounts for the decrease of pulse energy with the pump power. As mentioned by the authors, the pump absorption efficiency decreases from 90% to 74% when the incident pump power increases from 2 to 15.5 W. After assuming a moderate 80 mm distance between the pump spot and the absorber and calculating from their cavity configuration, the pump power reaching the Cr<sup>4+</sup>:YAG absorber in the 300  $\mu$ m mode radius varies in the range of 0.2 to 1.1 mW. Cr<sup>4+</sup>:YAG has a relatively high absorption at the 808 nm pump wavelength.<sup>10,11,21</sup>

Figure 2f in Ref. 8 described the increase–maximum–decrease in pulse energy with pump power in a cw-pumped Nd<sup>+</sup>:LaSc<sub>3</sub>(BO<sub>3</sub>)<sub>4</sub> (Nd<sup>+</sup>:LSB) microchip laser passively Q switched by Cr<sup>4+</sup>:YAG. The maximum value of pulse energy appears when the pump power is 0.8 W, corresponding to a 25 kHz pulse repetition frequency. When the pump power is lower than 0.8 W, or the pulse repetition frequency is lower than 25 kHz, pulse energy increases with pump power. When the pump power is larger than 0.8 W, or the pulse repetition frequency is larger than 25 kHz, pulse energy decreases fast with pump power. The pulse repetition frequency corresponding to the maximum value of pulse energy is 25 kHz. The increase of pulse energy with the pump power is attributed to some indirect modification to  $n_i$  via the thermal lens effect and subsequent loss in the gain medium and the absorber. Nevertheless, in this ex-

perimental configuration, the microchip Nd<sup>+</sup>:LSB and Cr<sup>4+</sup>:YAG are placed very close to keep the laser resonator very short. Despite the unabsorbed pump power, the considerable ASE fluorescence would be present during the recovery stage of the bleached Cr<sup>4+</sup>:YAG.

Therefore in these two investigations,<sup>7,8</sup> the occurrence of the illumination from the ASE and unabsorbed pump light would determine a finite recovery time of the bleached absorber. The increase–maximum–decrease in pulse energy with the pump power in these investigations show the coincidence with the low pump regime and high pump regime put forward in this paper. The finite recovery time  $T_s$  would be the interpulse period  $T$  at which the pulse energy reaches its maximum value when the pumping rate varies. Herein, by merging reported mechanisms<sup>7,8</sup> with our model, it would offer a comprehensive understanding to the increase–maximum–decrease of pulse energy with the pump power in a PQS laser.

#### B. Explanation to Morris and Pollock's Conclusion

In the investigation<sup>2</sup> on the cw diode-pumped Nd:YAG laser passively  $Q$  switched by a LiF:F<sub>2</sub><sup>-</sup> color center, when pump power increases from 420 to 630 mW, pulse energy keeps a constant value at 6 μJ (when  $T_0 = 94.8\%$ ), pulse repetition frequency increases from 2 to 8 kHz. And the corresponding interpulse period  $T$  within the range 500–125 μs, is 5000–1250 times larger than the spontaneous lifetime of LiF:F<sub>2</sub><sup>-2</sup>. For such a long interpulse period, before  $Q$  switching, the bleached LiF:F<sub>2</sub><sup>-</sup> recovers completely. Thus the case of this investigation follows the conclusion drawn for the low pump regime, i.e.,  $n_i$  remains constant,  $n_f$  decreases, while  $E$  increases monotonously with the pumping rate.

In Morris and Pollock's investigation, the photon energy at the pump wavelength is  $h\nu_p = 2.69 \times 10^{-19}$  J. As the gain medium, Nd:YAG's pump absorption cross section  $\sigma_{\text{abs}} = 8.63 \times 10^{-20}$  cm<sup>2</sup>, and the spontaneous emission lifetime of the Nd ion is  $\tau_{21} = 230$  μs. The TEM<sub>00</sub> mode area<sup>4</sup> is  $A = 0.153$  mm<sup>2</sup>. When the incident pump power  $P_{\text{in}} = 630$  mW, the maximum pump rate applied in this investigation is

$$W_p = \sigma_{\text{abs}} P_{\text{in}} / (h\nu_p A) = 132 \text{ s}^{-1}, \quad (29)$$

and  $W_p \tau_{21} = 0.03 \ll 1$ . Therefore in Ref. 2 the relative variation of pulse energy with the pumping rate,  $\partial E / \partial W_p$ , complies with Eq. (18), and primarily depends on the effect of the pump power to the final population density  $n_f$ , which finally is determined not only by the total dopant concentration  $N_t$ , but also the ratio of  $\tau_s / \tau_{21}$ , as emphasized in Subsection 3.A. The value of positive  $\partial E / \partial W_p$  increases with  $\tau_s / \tau_{21}$ .

Here we compare the value of the positive  $\partial E / \partial W_p$  when  $\tau_s$  varied under the condition of  $W_p \tau_{21} \ll 1$ . After assuming two Nd:YAG lasers passively  $Q$  switched by two different absorbers, Cr<sup>4+</sup>:YAG and LiF:F<sub>2</sub><sup>-</sup>, respectively, and according to Eq. (18), the values of derivative  $\partial E / \partial W_p$  for applying LiF:F<sub>2</sub><sup>-</sup> ab-

sorber is only nearly 1/50 of the counterpart for applying Cr<sup>4+</sup>:YAG absorber, i.e.,

$$\frac{\partial E}{\partial W_{P(\text{Cr}^{4+}:\text{YAG})}} \approx 50 \frac{\partial E}{\partial W_{P(\text{LiF:F}_2^-)}}. \quad (30)$$

Therefore Morris and Pollock's conclusion on the cw-pumped Nd:YAG/LiF:F<sub>2</sub><sup>-</sup> PQS laser, that pulse energy remains constant while pump power increases within the small range from 420 to 630 mW, is not only limited by the low pump range available at that time, but also by the relatively small excited state lifetime of the LiF:F<sub>2</sub><sup>-</sup> absorber.

## 6. Conclusions

In this paper we put forward the finite recovery time of the bleached absorber as a possible mechanism responsible for the increase–maximum–decrease in pulse energy with pump power for a cw-pumped passively  $Q$ -switched laser. This is done by analytically evaluating the sign of the derivative  $\partial E / \partial W_p$ . After defining the recovery time  $T_s$  of the bleached absorber and comparing it with interpulse period  $T$ , the operation of the passively  $Q$ -switched laser is divided into two regimes: low pump ( $T > T_s$ ), and high pump ( $T < T_s$ ), separated by a critical region ( $T \approx T_s$ ). The theoretical results show that, in the low pump regime,  $n_i$  remains constant and  $n_f$  decreases with  $W_p$ , resulting in a monotonic increase of pulse energy with  $W_p$ . When  $W_p \tau_{21} \ll 1$ , the value of  $\partial E / \partial W_p$  depends on the ratio of laser medium's upper level lifetime  $\tau_{21}$  to the absorber's excited state lifetime  $\tau_s$ . In the high pump regime,  $n_i$  decreases but  $n_f$  remains the same, resulting in a monotonic decrease of pulse energy with  $W_p$ . At the critical region, where the interpulse period is close to the full recovery time of absorber, the pulse energy reaches its maximum value.

We also pointed out the physical meaning of  $T_s$  in two aspects. First,  $T_s$  is some finite value (or range) larger than  $\tau_s$ , which keeps Eqs. (10a) and (10b) valid when  $T > T_s$  and Eqs. (14) and (15) valid when  $T < T_s$ . Second, the ASE fluorescence or unabsorbed pump power also gives the possibility of the finite recovery time since such illumination could enhance the equilibrium population on the excited state of two-level absorber.

To confirm our analytical model, a cw-pumped Yb:YAG laser  $Q$  switched by a Cr<sup>4+</sup>:YAG absorber was demonstrated. Thereafter we mentioned the occurrences of the ASE fluorescence and unabsorbed pump power in the Cr:YAG in two PQS solid-state (Nd:GdVO<sub>4</sub>, Nd:LSB) lasers experiments reported previously, and also revisited Morris and Pollock's conclusion in the light of our model.

It is worthwhile to mention that our theoretical model gives out a general description to the increase–maximum–decrease in pulse energy, which has been noted by other authors. However, we don't think our model governs over other mechanisms.<sup>7,8</sup> A further model for full explanations of such (extremum) behavior should also include the effect of lasing mani-

folds, thermalization rate, and the lower lasing level decay time, and also the excited state absorption of the absorber. Especially in the passively  $Q$ -switched Nd:YAG microchip laser with subnanosecond to picosecond pulse width, the thermalization and lower level decay time become important for the dynamics of  $Q$  switching.

As the functions of the pump power, the remaining variables for describing the  $Q$ -switched pulse are the peak power  $P_{\max}$  and pulse width  $t_p$ . The theoretical investigations on the extrema phenomena on the function relations of  $P_{\max} \sim W_p$  and  $t_p \sim W_p$  are not determined at this moment because their respective expressions of  $P_{\max}$  and  $t_p$  are much more complicated than the case of  $E$ . We would try to seek a new mathematical method to obtain an intuitive insight into this issue, as the way treating the pulse energy  $E$  in this paper.

The authors acknowledge Kazunori Takaichi for his helps in the preparation of Yb:YAG ceramics. J. Li also appreciates the helpful discussion from S. V. Voitikov and J.-F. Bisson. J.-F. Bisson also put much effort into enhancing the English of this paper.

## References

1. B. Braun, F. X. Kartner, G. Zhang, M. Moser, and U. Keller, "56-ps passively  $Q$ -switched diode-pumped microchip laser," *Opt. Lett.* **22**, 381–383 (1997).
2. J. A. Morris and C. R. Pollock, "Passive  $Q$  switching of a diode-pumped Nd:YAG laser with a saturable absorber," *Opt. Lett.* **15**, 440–442 (1990).
3. J. J. Degnan, "Theory of the optimally coupled  $Q$ -switched laser," *IEEE J. Quantum Electron.* **25**, 214–220 (1989).
4. J. J. Degnan, "Optimization of passively  $Q$ -switched lasers," *IEEE J. Quantum Electron.* **31**, 1890–1901 (1995).
5. G. Xiao and M. Bass, "A generalized model for passively  $Q$ -switched laser including excited state absorption in the saturable absorber," *IEEE J. Quantum Electron.* **33**, 2286–2294 (1997).
6. W. Koechner, *Solid State Laser Engineering*, 4th ed. (Springer-Verlag, 1996).
7. J. Liu, B. Ozygus, S. Yang, J. Erhard, U. Seelig, A. Ding, H. Weber, X. M. L. Zhu, L. Qin, C. Du, X. Xu, and Z. Shao, "Efficient passive  $Q$ -switching operation of a diode-pumped Nd:GdVO<sub>4</sub> laser with a Cr<sup>4+</sup>:YAG saturable absorber," *J. Opt. Soc. Am. B* **20**, 652–661 (2003).
8. S. V. Voitikov, A. A. Demidovich, L. E. Batay, A. N. Kuzmin, and M. B. Danailov, "Sub-nanosecond pulse dynamics of Nd:LSB microchip laser  $Q$ -switched by Cr:YAG saturable absorber," *Opt. Commun.* **251**, 154–164 (2005).
9. D. Welford, "Passively  $Q$ -switched lasers: short pulse duration, single-frequency sources," *Proceedings of Lasers and Electro-Optics Society Annual Meeting* (Institute of Electrical and Electronics Engineers, Piscataway, N.J., 2001), pp. 121–122.
10. J. J. Zayhowski and A. L. Wilson, "Pump-induced bleaching of the saturable absorber in short-pulse Nd:YAG/Cr<sup>4+</sup>:YAG passively  $Q$ -switched microchip lasers," *IEEE J. Quantum Electron.* **39**, 1588–1593 (2003).
11. M. A. Jaspán, D. Welford, and J. A. Russell, "Passively  $Q$ -switched microlaser performance in the presence of pump-induced bleaching of the saturable absorber," *Appl. Opt.* **43**, 2555–2560 (2004).
12. X. Zhang, S. Zhao, Q. Zhang, L. Sun, and S. Zhang, "Optimization of Cr<sup>4+</sup>-doped saturable-absorber  $Q$ -switched laser," *IEEE J. Quantum Electron.* **33**, 41–44 (1997).
13. P. Peterson, A. Gavrielides, M. P. Sharma, and T. Erneux, "Dynamics of passively  $Q$ -switched microchip lasers," *IEEE J. Quantum Electron.* **35**, 1247–1256 (1999).
14. J. J. Degnan, D. B. Coyle, and R. B. Kay, "Effect of thermalization on  $Q$ -switched laser properties," *IEEE J. Quantum Electron.* **32**, 887–899 (1998).
15. A. Szabo and R. A. Stein, "Theory of laser giant pulsing by a saturable absorber," *J. Appl. Phys.* **36**, 1562–1566 (1965).
16. W. G. Wagner and B. A. Lengyel, "Evolution of giant pulse in a laser," *J. Appl. Phys.* **34**, 2040–2046 (1963).
17. X. Zhang, S. Zhao, Q. Wang, Y. Liu, and J. Wang, "Optimization of dye  $Q$ -switched lasers," *IEEE J. Quantum Electron.* **30**, 905–908 (1994).
18. R. Herda and O. G. Okhotnikov, "Effect of amplified spontaneous emission and absorber mirror recovery time on the dynamics of mode-locked fiber lasers," *Appl. Phys. Lett.* **86**, 011113 (2005).
19. Z. G. Li, Z. J. Xiong, N. Moore, G. C. Lim, W. L. Huang, and D. X. Huang, "Amplified-spontaneous-emission effects in a passively  $Q$ -switched diode-pumped Nd:YVO<sub>4</sub> laser," *J. Opt. Soc. Am. B* **21**, 1479–1485 (2004).
20. G. J. Quarles, "Comparison of ceramic lasers with single crystal materials," presented at Photonics West on Lasers and Applications in Science and Engineering, San Jose, California, 22–27 January 2005.
21. Z. Burshtein, P. Blau, Y. Kalisky, Y. Shimony, and M. R. Kokta, "Excited-state absorption studies of Cr<sup>4+</sup> ions in several garnet host crystals," *IEEE J. Quantum Electron.* **34**, 292–299 (1998).